

## Diffusion in a periodically driven damped and undamped pendulum

R. Harish,<sup>1</sup> S. Rajasekar,<sup>2</sup> and K. P. N. Murthy<sup>3</sup>

<sup>1</sup>Reactor Physics Division, Indira Gandhi Centre for Atomic Research, Kalpakkam 603 102, Tamil Nadu, India

<sup>2</sup>Department of Physics, Manonmaniam Sundaranar University, Tirunelveli 627 012, Tamil Nadu, India

<sup>3</sup>Materials Science Division, Indira Gandhi Centre for Atomic Research, Kalpakkam 603 102, Tamil Nadu, India

(Received 25 May 2001; revised manuscript received 26 November 2001; published 3 April 2002)

We study the diffusion process in a periodically driven damped and undamped pendulum. The effect of angular frequency  $\omega$  of the external periodic force on the diffusion process is investigated. We show the occurrence of normal and anomalous diffusions in the undamped system. In the presence of damping, normal chaotic diffusion is found. Near certain bifurcation points, the phase velocity is found to be intermittent and the diffusion coefficient is found to exhibit power-law divergence. We argue that the divergence of the diffusion coefficient near the bifurcation points is similar to that of the average laminar lengths near them. The effect of bias on the dynamics is also discussed.

DOI: 10.1103/PhysRevE.65.046214

PACS number(s): 05.45.-a, 02.50.Ey, 74.40.+k

### I. INTRODUCTION

The diffusion process is usually broadly classified as normal and anomalous. The characteristic of diffusion is based on the time evolution of the mean-square displacement  $\langle R^2(t) \rangle \sim t^\mu$ . If  $\mu = 1$ , the process is called normal and if  $\mu \neq 1$ , the process is called anomalous. The anomalous diffusion process can further be categorized into sub (linear) diffusion when  $\mu < 1$  and super (linear) diffusion or enhanced diffusion when  $\mu > 1$ . See Refs. [1–4] for an exhaustive review of normal and anomalous diffusion processes. Anomalous diffusion is of basic interest in several problems such as mass transport and mixing in hydrodynamic flows [5–7], transport of magnetic field lines, and heat and particles in fusion and space plasmas [8–10] to name only a few. Of late there has been a growing interest in the diffusion properties of chaotic systems. There have been several studies devoted to normal and anomalous diffusion in maps and continuous time systems [11–13]. Anomalous diffusion is found to occur in several conservative systems, especially, when the domain of chaotic motion has accelerator modes or when stochastic layers form near the unperturbed separatrix. For example, it has been found in a model of electrostatic turbulent plasma [14] and in certain Hamiltonian systems and maps [15–20]. In these systems, an orbit gets trapped in the accelerator modes resulting in ballistic motion during these trapped times and moves chaotically otherwise. The combination of this regular and chaotic motion leads to anomalous (non-Brownian) diffusion. In this paper, we shall focus attention on diffusion in the driven damped and undamped classical pendulum equation. The driven damped pendulum is a classical nonlinear system that is used to model many physical phenomena such as charge-density wave transport and radio frequency driven Josephson junction. Recently, diffusion process has been studied in a damped and periodically driven pendulum [21–23]. Superdiffusion in an equivalent equation was studied by Latora *et al.* [24]. The equation of motion of a sinusoidally forced, damped pendulum with constant bias is given by

$$\ddot{\theta} + \gamma \dot{\theta} + \sin \theta = f \sin(\omega t) + p. \quad (1)$$

One can view the motion of the pendulum bob about the pivot as an evolving trajectory in the phase plane  $(\theta, \dot{\theta})$ . The dynamics of the system (1) for  $p=0$  has been studied by a number of authors [21,22]. For certain range of values of the parameters the evolution of the phase variable  $\theta$  shows expansion behavior characteristic of classical diffusion. The diffusion properties of the pendulum equation were studied by Blackburn and Jensen [21], where the diffusion was calculated as a function of  $\gamma$ . It was found by them that the diffusion coefficient exhibits a power-law divergence,  $|\gamma - \gamma_c|^{-1/2}$ , outside a periodic window of  $\gamma$ . Popescu *et al.* [22] considered the system (1) with disorder substrate and  $p=0$ . They added, quenched disorder  $\alpha \xi(\theta)$  to the right side of Eq. (1), where  $\alpha$  is the amount of quenched disorder and the random variable  $\xi(\theta) \in [-1, 1]$  obeys

$$\langle \xi(\theta) \rangle = 0, \quad \langle \xi(\theta) \xi(\theta') \rangle = \delta(\theta, \theta'). \quad (2)$$

They found that the diffusion coefficient increases with the strength of disorder  $\alpha$ , when  $\alpha$  is small. However, when disorder strength is very high, the diffusion coefficient becomes very small. More recently, Yevtushenko, Flach, and Richter [23] reported on the dependence of mean velocity on the phase of the periodic driving force in the undamped system. Directed current due to broken time-space symmetry was also reported in Ref. [25]. In the present paper, we study the diffusion in Eq. (1) with (i)  $p=0$ ,  $\gamma=0$  and (ii)  $p=0$ ,  $\gamma \neq 0$ . We focus on the effect of the parameters  $\omega$ . When  $\gamma = 0$  and  $p=0$ , the system exhibits normal and anomalous diffusion depending upon the values of  $f$  and  $\omega$ . The diffusion process is characterized using various statistical descriptors. We also investigate the damped pendulum by setting  $\gamma=0.2$ ,  $f=1.2$ ,  $p=0$ , and varying  $\omega$ . Diffusion, when it occurs is found to be normal in the damped system. We present results on the variation of diffusion coefficient near two bifurcation points  $\omega_1$  and  $\omega_2$  shown in Fig. 5. We show power-law divergence of the diffusion coefficient as the control parameter  $\omega$  is varied near these bifurcations. We also study the diffusion behavior near a bifurcation leading to the crisis induced intermittency. Finally, we study the effect of the constant bias  $p$  on the dynamical evolution.

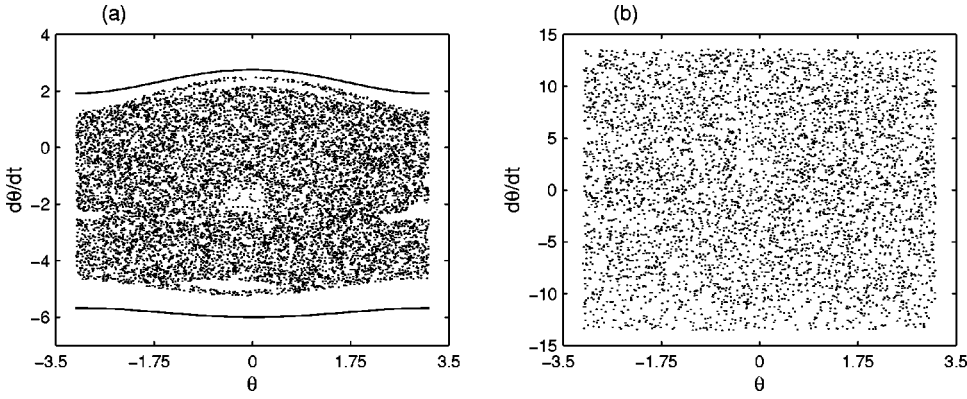


FIG. 1. Poincaré map of Eq. (1) for  $p=0$ ,  $\gamma=0$ , and  $f=1.2$ . (a)  $\omega=0.8$ . (b)  $\omega=0.1$ . The points on the Poincaré map are sampled once every drive period with phase  $\phi=0$  for (a) and  $\phi=0.25\omega$  for (b).

**II. DIFFUSION IN THE CONSERVATIVE SYSTEM**  
( $\gamma=0, p=0$ )

For  $f=\gamma=p=0$ , the system has two equilibrium points:  $(\theta^*, \dot{\theta}^*)=(0,0)$ , which is an elliptic point and the joining of the two branches of the separatrix at  $(\pm\pi,0)$ , which is a hyperbolic point. For nonzero values of these parameters, it is not possible to obtain analytical solutions and one is forced to take recourse to the numerical evaluation of the trajectories. For the generation of the numerical trajectories a fourth-order fixed time step Runge-Kutta integrator was used. All the calculations were carried out in double precision arithmetic. An optimum choice of 100 time steps per drive cycle was found to give satisfactory results for calculating statistical quantities such as the diffusion coefficient. This choice of the time step was used in the case of damped system. For the undamped system, however, we used a smaller value, 5000 time steps per drive cycle [26]. Figure 1(a) shows the Poincaré map for  $\gamma=0, p=0, f=1.2$ , and  $\omega=0.8$ . The Poincaré map is plotted by sampling the trajectory once per drive cycle. In Fig. 1(a), orbits for three different initial conditions are shown. The upper and lower orbits are quasiperiodic, while the middle one is chaotic. The accelerator islands are clearly visible. The phase plot for the case  $\omega=0.1$  is shown in Fig. 1(b). The difference in the nature of the distribution of points contribute to the different diffusion behavior. For  $\omega=0.8$ , both laminar and chaotic flows can be seen in Fig. 2(a). When the trajectory spends a long duration of time on a stochastic layer the phase velocity  $\dot{\theta}$  appears laminar. In Fig. 2(b), in the laminar regions where  $\dot{\theta}$  is nearly constant, the phase variable  $\theta$  increases or decreases linearly. After escape from a stochastic layer the trajectory wanders chaotically. In the bursting region, the phase velocity  $\dot{\theta}$  rapidly oscillates. The combination of these two motions lead to anomalous diffusion. To identify and characterize the nature of diffusion in the system Eq. (1), we calculated various statistical quantities. The mean-square displacement  $\langle \theta^2(n) \rangle$ , was calculated by averaging over 1520 initial conditions chosen around the origin ( $\theta=0, \dot{\theta}=0$ ) of the phase space. Figure 3 depicts the variation of  $\langle \theta^2(n) \rangle$  as a function of  $n$ , the number of drive cycles, for  $\omega=0.8$  and  $\omega=0.1$ . The data points for both the values of  $\omega$  in the log-log plot asymptotically fall on straight lines implying the relation

$$\langle \theta^2(n) \rangle \sim n^\mu, \quad n \rightarrow \infty. \quad (3)$$

For  $\omega=0.8$ , the exponent  $\mu$  is found to be 1.6, which implies that the diffusion process is anomalous, and superlinear. For  $\omega=0.1$ , the exponent  $\mu$  is evaluated by a least squares fit for  $n > 500$ .  $\mu$  is unity and hence asymptotically the diffusion is normal. A simple way to check whether a one-dimensional random variable  $\theta$  with zero mean is Gaussian or not is to calculate the magnitude of the fourth cumulant

$$C_4 = \langle \theta^4 \rangle - 3\langle \theta^2 \rangle^2. \quad (4)$$

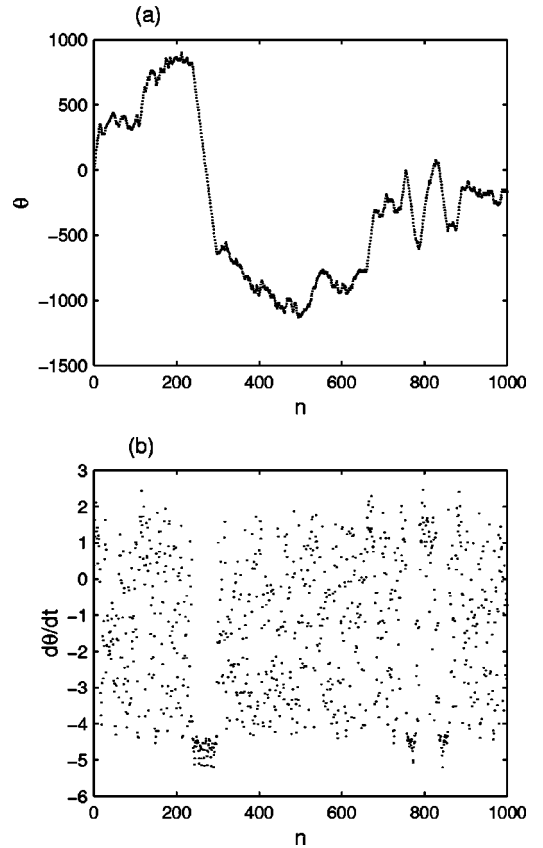


FIG. 2. Phase variables  $\theta$  (a) and  $\dot{\theta}$  (b) for a trajectory started near the origin for  $\omega=0.8, \gamma=0, p=0$ , and  $f=1.2$ . The linear motion of  $\theta$  during the laminar phases of  $\dot{\theta}$  is evident.

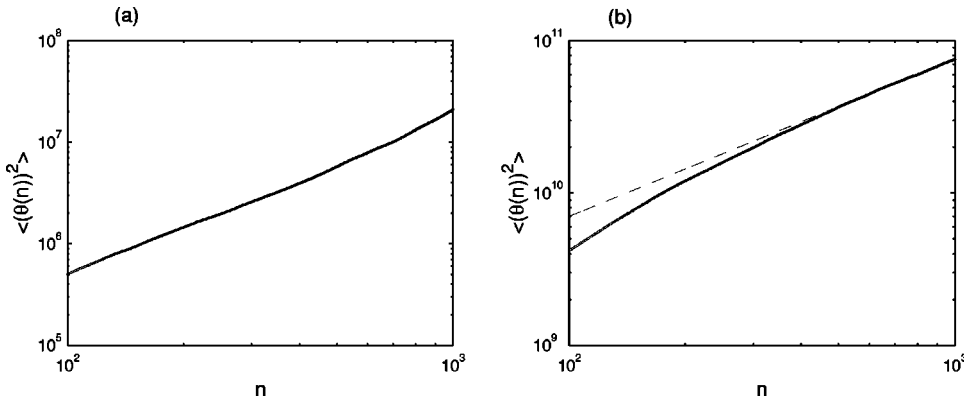


FIG. 3. Diffusion for the case of Fig. 1. (a)  $\omega=0.8$ . The diffusion is anomalous with  $\mu=1.6$ . (b)  $\omega=0.1$ . The diffusion is normal asymptotically. The dashed line is the least squares fit for  $n$  between 500 and 1000. The exponent  $\mu$  is nearly unity.

For Gaussian process,  $C_4$  and other higher-order cumulants vanish. Deviation from Gaussian process can be measured by evaluating the kurtosis

$$K = \frac{\langle \theta^4 \rangle}{\langle \theta^2 \rangle^2}. \tag{5}$$

When the diffusion is Gaussian the value of kurtosis is expected to be nearly 3. Figure 4 shows the variation of  $K$  for  $\omega=0.1$  and  $\omega=0.8$ , respectively. For  $\omega=0.1$ ,  $K$  is found to be nearly 3 for large  $n$  confirming normal diffusion. For  $\omega=0.8$ ,  $K$  diverges rapidly with  $n$  implying deviation from Gaussian statistics.

### III. DIFFUSION IN THE DAMPED AND PERIODICALLY DRIVEN SYSTEM ( $p=0, \gamma \neq 0$ )

In this section, we consider the system (1) in the presence of damping with  $p=0, f=1.2$ , and  $\gamma=0.2$ , and study the diffusion process by varying the angular frequency  $\omega$  of the

external force. The periodic orbits of the system (in the phase variable  $\theta$ ) are either running or nonrunning, depending on the value of the parameter  $\omega$ . A typical running orbit shows expansion of the phase variable  $\theta$  with time, while a nonrunning orbit does not.

First, we consider chaotic diffusion resulting from the bifurcation of a running periodic orbit. Figure 5 shows the bifurcation diagram for  $\omega \in (0.471, 0.477)$ . As  $\omega$  is decreased there is a sequence of period doubling bifurcations. At the accumulation point of these bifurcations,  $\omega_1 = 0.47315 \dots$ , the attractor suddenly widens. The region to the left of this point is interesting. A typical trajectory in this region of  $\omega$  exhibits a succession of laminar regions in  $\theta$  interrupted by chaotic bursts. In fact, there are two laminar regions and in each of these regions, the phase variable  $\theta$  is linear. While on one of these  $\theta$  increases, on the other  $\theta$  decreases. During the chaotic bursts, the net displacement is small. Figures 6(a) and 6(b) show the laminar and chaotic regions for  $\omega = 0.4731475$ , which is close to  $\omega_1$ . Figure 6(a) shows the variation of  $\theta$  on the Poincaré surface. The evolution of  $\dot{\theta}$  on

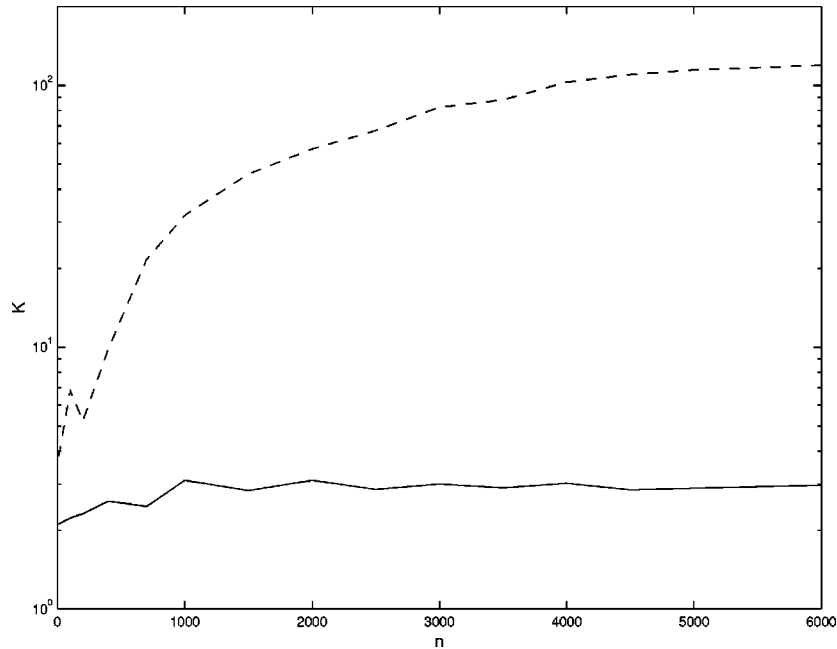


FIG. 4. Kurtosis for the undamped driven pendulum. For  $\omega=0.8$  exhibiting anomalous diffusion  $K$  diverges (dotted line), and for  $\omega=0.1$  exhibiting normal diffusion  $K$  is nearly 3 (solid line).

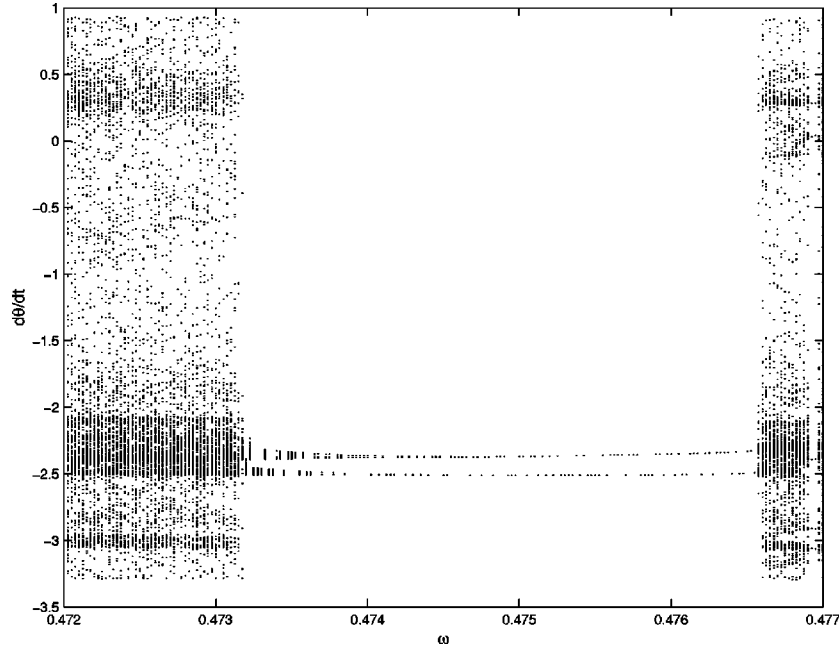


FIG. 5. Bifurcation diagram of the system (1) for  $\omega \in (0.471, 0.477)$ . The period 1 orbit suddenly becomes chaotic at  $\omega = 0.476571\dots$ . There is a sequence of period doubling bifurcations as  $\omega$  is decreased. The attractor suddenly widens at  $\omega = 0.47315\dots$ .

the Poincaré section is shown in Fig. 6(b). The correspondence between the laminar regions of  $\dot{\theta}$  in Fig. 6(b) and the ballistic motion of  $\theta$  in Fig. 6(a) is clear. The diffusion coefficient  $D$  is defined by

$$D = \lim_{n \rightarrow \infty} \frac{1}{n} \langle \theta^2(n) \rangle. \quad (6)$$

$D$  is calculated by evolving 2600 trajectories with initial conditions around the origin for 2000 drive cycles in the region  $\omega \in (0.47125, 0.47314)$ . The nature of diffusion is found to be normal. For  $\omega$  close to the critical points, longer trajectories are required for observing normal diffusion. Figure 7(a) shows the linear evolution of the mean-square displacement for  $\omega = 0.47314$ . The contribution to the diffusion is primarily due to the ballistic motion in the laminar regions. The burst regions contribute only minimally. The diffusion coefficient  $D$  exhibits a power-law divergence  $D \sim |\omega - \omega_1|^{-\alpha}$  with  $\alpha = 0.492$  and is shown in Fig. 7(b). As  $\omega$  is increased through the periodic window, the motion becomes suddenly chaotic at  $\omega_2 = 0.476571\dots$ . After this bifurcation point, the behavior is somewhat similar to that found for Fig. 6. There are two distinct laminar regions in which the motion is ballistic. The laminar regions and chaotic bursts are shown in Figs. 8(a) and 8(b). Normal diffusion at  $\omega = 0.47658$  is shown in Fig. 9(a) and the power-law divergence of the diffusion coefficient in the region  $\omega \in (0.47658, 0.47670)$  is shown in Fig. 9(b). The exponent  $\alpha$ , in this case is 0.483. The value of the exponent seems to be 1/2. Several similar bifurcations lead to divergence of the diffusion coefficient with the same exponent. For example, for  $\gamma = 0.15$ ,  $f = 1.2$ ,  $p = 0$ , and  $\omega = 0.489856\dots$ , we found the value of the exponent to be 0.526. At the same parameters but with  $\omega$

$= 0.49288486\dots$ , we found the value of the exponent to be 0.48. Blackburn and Jensen [21] also found that the exponent is 1/2 in their studies.

We studied the variation of diffusion coefficient just after another type of bifurcation called the crisis induced intermittent switching between two chaotic orbits. This type of bifurcation was studied by Grebogi *et al.* [27] in the system

$$\ddot{\theta} + \gamma \dot{\theta} + \sin \theta = f \cos(\omega t). \quad (7)$$

In this type of intermittency, there exist two attractors, one with  $\dot{\theta} < 0$  on the average and another with  $\dot{\theta} > 0$  on the average with their respective basins of attraction. That the existence of one attractor implies the existence of the other follows from the symmetry of the equation. Let  $f_c$  be the bifurcation point. For  $f < f_c$ , the orbit is in one of the attractors depending on which basin of attraction the initial condition was in. After  $f$  crosses  $f_c$ , the two basins of attractions merge and form a single large attractor. The orbit then switches between the two attractors chaotically. That is, the system exhibits

$$(\text{chaos})_1 \rightarrow (\text{chaos})_2 \rightarrow (\text{chaos})_1 \rightarrow (\text{chaos})_2 \rightarrow \dots$$

transition [27]. They showed that the mean time between switching as a function of  $f - f_c$  is power law, where the exponent is given in terms of the expanding and contracting eigenvalues. We found that the diffusion is normal and determined the diffusion coefficient for this system ( $\omega = 1.0$ ,  $\gamma = 0.22$ ,  $p = 0$ ,  $f_c = 2.646442$ ) as a function of  $f - f_c$  [28]. The diffusion coefficient was calculated in the region  $f \in (2.64653, 2.69)$ . The divergence of the diffusion coeffi-

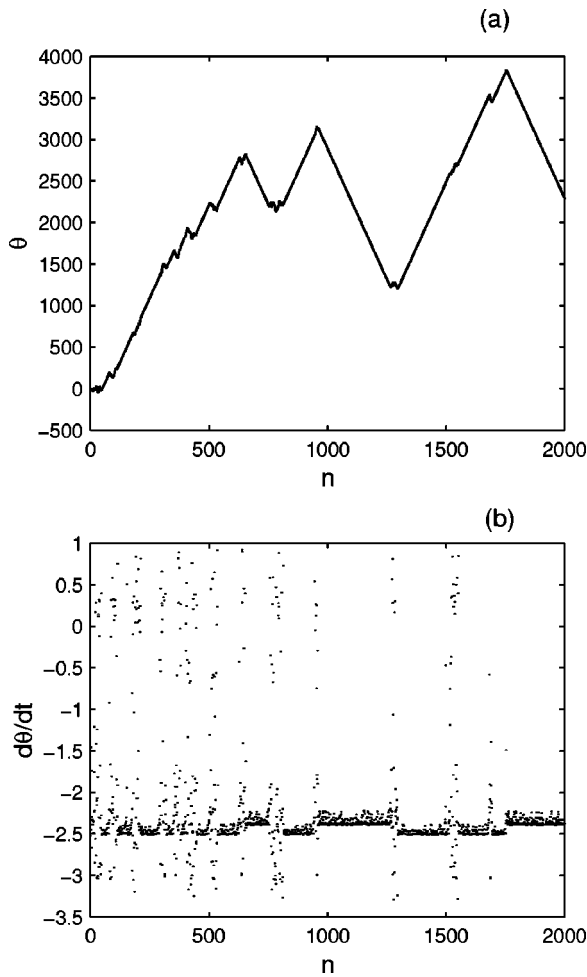


FIG. 6. Intermittency near the bifurcation at  $\omega = 0.47315 \dots$ . (a) The evolution of the phase variable  $\theta$  on the Poincaré surface at  $\omega = 0.4731475$ . (b) The phase velocity on the Poincaré surface. The linear evolution and small chaotic oscillations of  $\theta$  in (a) correspond to the laminar regions and the burst regions, respectively, in (b).

cient is power law with the exponent 0.699. Intermittency and divergence of the diffusion coefficient for this case are shown in Fig. 10.

We wish to find a possible explanation for the value of the exponent 1/2 for the diffusion near the bifurcation values  $\omega_{1,2}$ . Figure 6 shows  $\theta(n)$ ,  $\dot{\theta}(n)$  for  $\omega = 0.4731475$  near

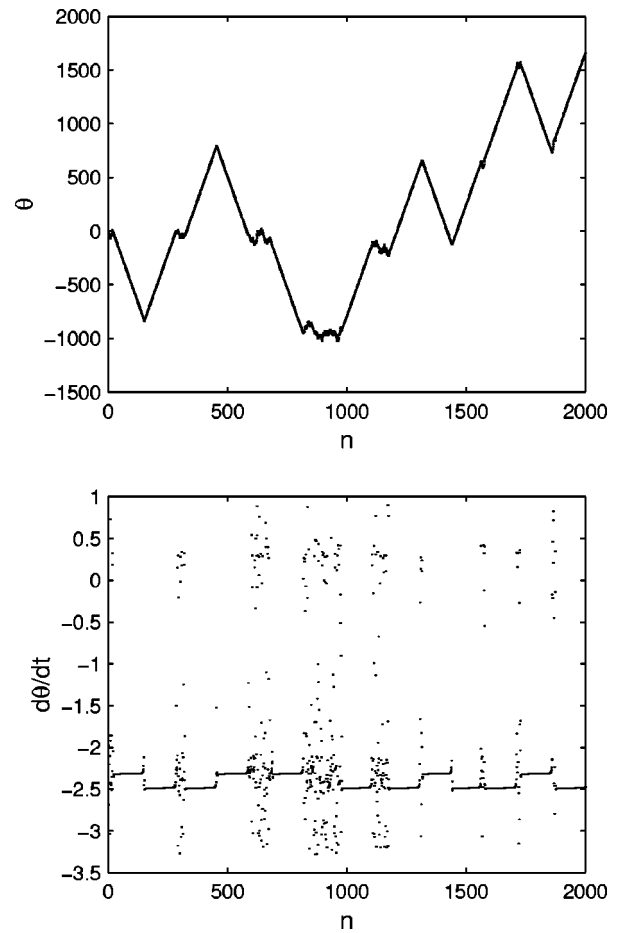


FIG. 8. Intermittency near the bifurcation point at  $\omega = 0.476571 \dots$ . (a) The evolution of the phase variable  $\theta$  on the Poincaré surface at  $\omega = 0.476572$ . (b) The phase velocity on the Poincaré surface. The linear evolution and small chaotic oscillations of  $\theta$  in (a) correspond to the laminar regions and the burst regions, respectively, in (b). The linearly increasing and decreasing values of  $\theta$  correspond to the two distinct laminar regions as seen in (b).

$\omega_1$ . The trajectory spends long time intervals in the regions where  $\dot{\theta}(n)$  is nearly constant on the Poincaré map, akin to the laminar regions, interrupted by bursts. In these regions, the trajectory is linear as seen in Fig. 6(a). In the bursting regions  $\dot{\theta}$  fluctuates rapidly giving rise to small amplitude motion of  $\theta$ . Consequently, the displacement in these regions

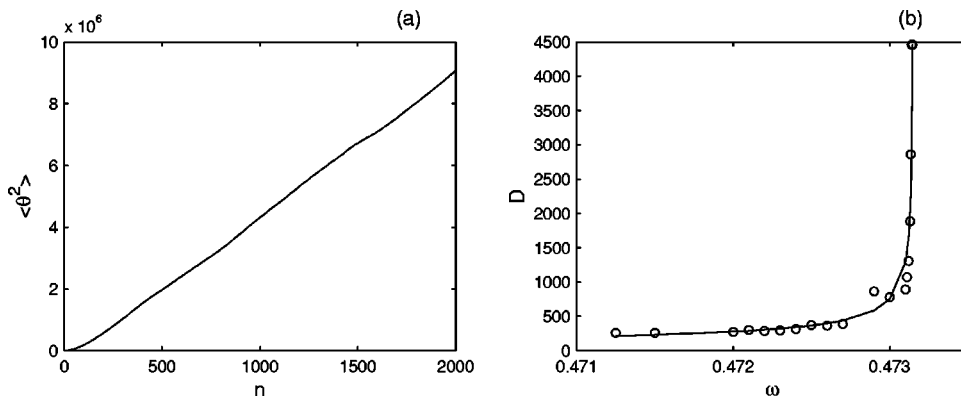


FIG. 7. (a) Mean-square displacement showing normal diffusion for  $\omega = 0.47314$ . (b) Diffusion coefficient near the bifurcation point showing power-law behavior for  $\omega \in (0.47125, 0.47314)$ . Circles represent the numerically evaluated values and the solid line is the least squares fit.

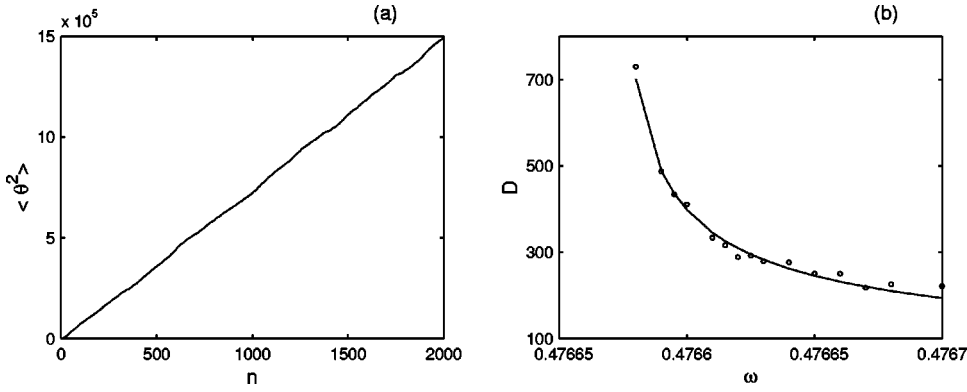


FIG. 9. (a) Mean-square displacement showing normal diffusion for  $\omega = 0.47658$ . (b) The diffusion coefficient near the bifurcation showing power law. Circles represent numerically evaluated values and the solid line is the least squares fit.

is much smaller as compared to those in the laminar regions. When  $\omega$  is decreased, the average length of the regions where  $\dot{\theta}$  is laminar decreases and diffusion slows down. We have found numerically that the average laminar length near the critical point  $\omega_1$  exhibits power-law divergence  $\langle l \rangle \sim |\omega_1 - \omega|^{-\alpha}$  with  $\alpha = 0.437$  as seen in Fig. 11(b). The laminar length  $l$  is found to be random with exponential distribution see Fig. 11(a). The distribution is obtained by collecting successive laminar lengths for a long orbit and binning them appropriately. The log-linear plot exhibiting linear behavior is taken as the signature of the exponential distribution.

Let us consider the process close to the critical point. The evolution of  $\theta$  as a function of time is dominated by laminar regions interrupted by chaotic bursts. The change in  $\theta$  during a chaotic burst is small compared to that during a laminar region. Hence, neglecting the small displacements in the burst regions, the net displacement of  $\theta$  in time  $n$  can be written as a sum of the displacements  $\zeta_i$  in the laminar regions of length  $l_i$ ,

$$\theta(n) = \sum_{i=1}^N \zeta_i(l_i), \quad (8)$$

where  $N$  is the number of laminar regions between time zero and  $n$ .  $\zeta_i$  are the independent random displacements that take positive and negative values with equal probability. The mean-square displacement  $\langle \theta^2 \rangle$  can, therefore, be written as

$$\langle \theta^2(n) \rangle = N \langle \zeta^2 \rangle, \quad (9)$$

where  $\langle \zeta^2 \rangle$  is the mean-square displacement per step. In the laminar regions,  $\dot{\theta}$  is nearly constant on the Poincaré surface. Figure 6 shows the two laminar regions and the corresponding linear motion of  $\theta$ . The two laminar regions are symmetrical leading to zero average velocity, which is not evident in the figure due to the choice of the Poincaré surface. Hence,  $\zeta_i \sim a l_i$ ,  $\zeta_i^2 \sim a^2 l_i^2$ . The quantity  $a$  represents the average velocity in the laminar regions and can take values of the same magnitude and opposite signs in the two different regions. The problem of determining the mean-square displacement, therefore, reduces to determining the mean-square laminar length [29]. Since, the laminar length has an exponential distribution, the probability for finding laminar regions of length between  $l$  and  $l + dl$  can then be written as  $(1/\langle l \rangle) \exp(-l/\langle l \rangle)$ , where  $\langle l \rangle$  is the average laminar length. The factor  $1/\langle l \rangle$  provides the correct normalization. The mean-square laminar length can be then written as

$$\langle l^2 \rangle = \frac{1}{\langle l \rangle} \int_0^\infty l^2 \exp\left(-\frac{l}{\langle l \rangle}\right) dl = 2 \langle l \rangle^2. \quad (10)$$

Hence,  $\langle \zeta^2 \rangle \sim \langle l^2 \rangle = 2 \langle l \rangle^2$ . In time  $n$ , the number of laminar lengths is  $N = n/\langle l \rangle$ . Substituting this in Eq. (9), we get

$$\langle \theta^2(n) \rangle \sim \langle l \rangle n. \quad (11)$$

The above implies that the diffusion coefficient is proportional to the mean laminar length.

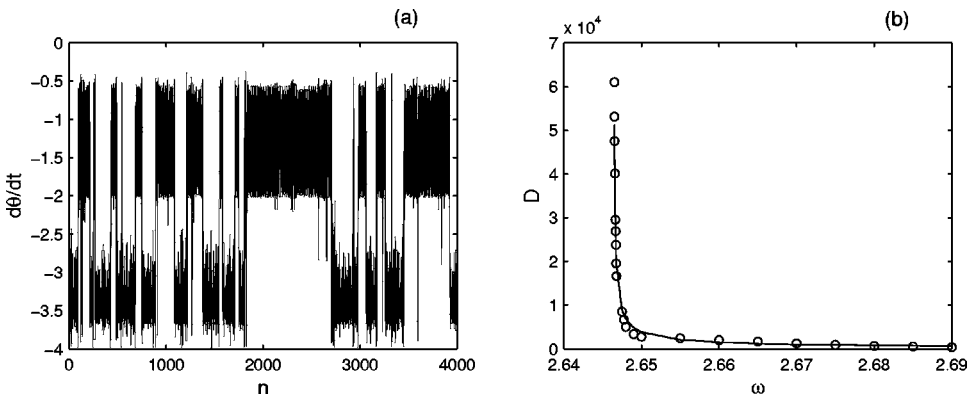


FIG. 10. Crisis induced intermittency in the damped driven pendulum for the parameters  $\omega = 1$ ,  $\gamma = 0.22$ , and  $p = 0$ . (a) Intermittency for  $f = 2.655$ . (b) Diffusion coefficient near the bifurcation point showing power-law behavior.  $D$  is calculated in the range  $f = (2.64653, 2.69)$ . Circles represent the numerically evaluated values and the solid line is the least squares fit.

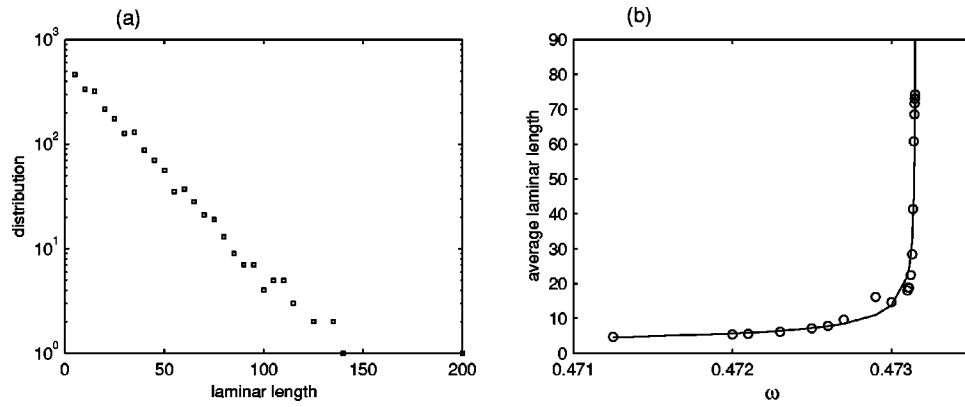


FIG. 11. Distribution (a) and divergence (b) of laminar lengths for the damped driven pendulum with  $p=0$ ,  $f=1.2$ , and  $\gamma=0.2$ . The distribution is obtained by binning 2185 laminar lengths in bins of width 5 drive cycles after removing “laminar” regions of very small lengths. The linearity on the log-linear plot indicates that the distribution is exponential. The divergence of the laminar lengths is power law with exponent 0.437.

The mean laminar length exhibits power-law divergence near the critical points of  $\omega$  as shown in Fig. 7(b) and Fig. 9(b). We have observed numerically that the exponent  $\alpha$  in the power law is nearly  $1/2$ . In this connection we add that in many systems near such bifurcation points the mean value of state variables and maximal Lyapunov exponent have shown similar power-law dependence on a control parameter [30,31]. This also is probably the reason for the power-law divergence (with exponent  $1/2$ ) observed by Blackburn and Jensen [21]. If we are away from the critical points, the ballistic motion in the laminar regions and the motion in the chaotic burst regions become comparable and the above random walk arguments do not hold good any more.

In the case of the crisis induced intermittency, the average laminar length exhibits power-law divergence with exponent 0.702 [27]. We have found that the laminar length distribution is exponential. As in the previous case, by invoking the random walk argument, it is reasonable to expect similar divergence for the diffusion coefficient.

Now, we consider the pendulum equation (1) with bias,  $p \neq 0$ . For the choice of parameters  $f=1.2$ ,  $\gamma=0.2$ ,  $\omega=0.4769$ , and  $p=0$ , the system is periodic. For  $p \neq 0$ , the system loses its periodicity. The resulting bifurcation diagram is shown in Fig. 12. The system is alternately chaotic and periodic with increasing  $p$ , chaoticity emerging through a series of period doubling bifurcations. The phase velocity

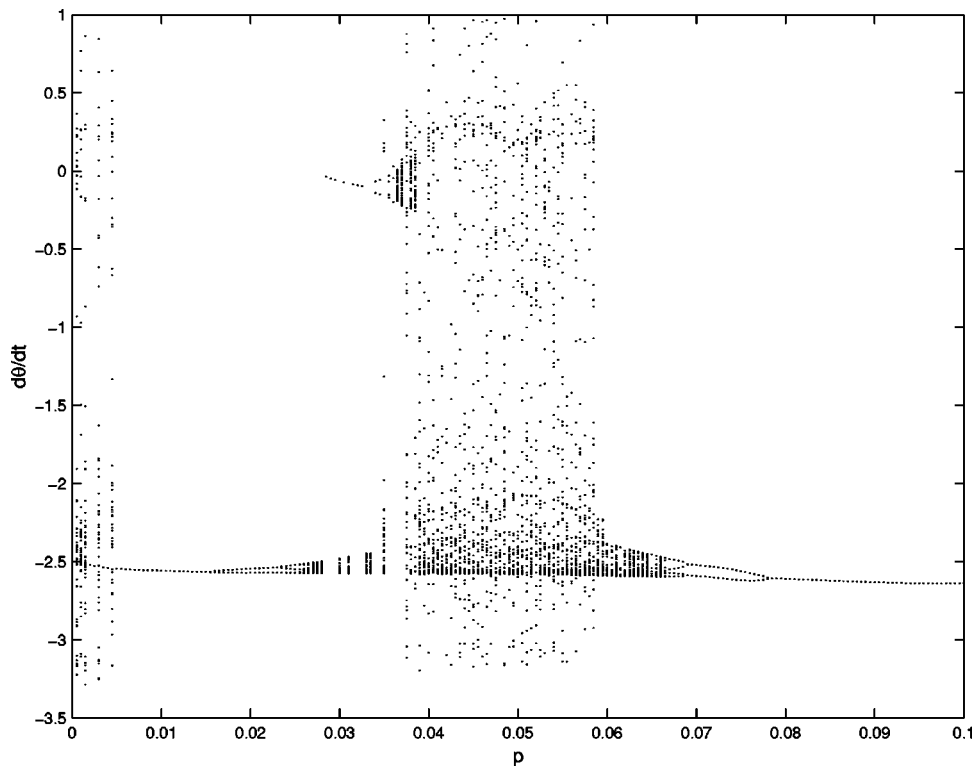


FIG. 12. Bifurcation diagram for the damped driven pendulum with bias,  $\omega=0.4769$ ,  $f=1.2$ , and  $\gamma=0.2$ . The periodic state that exists for  $p=0$  loses its periodicity and becomes chaotic. Subsequently for higher values of  $p$ , there is a sequence of chaotic and periodic regions. The chaotic region contain a single intermittent region where the motion is nearly linear.

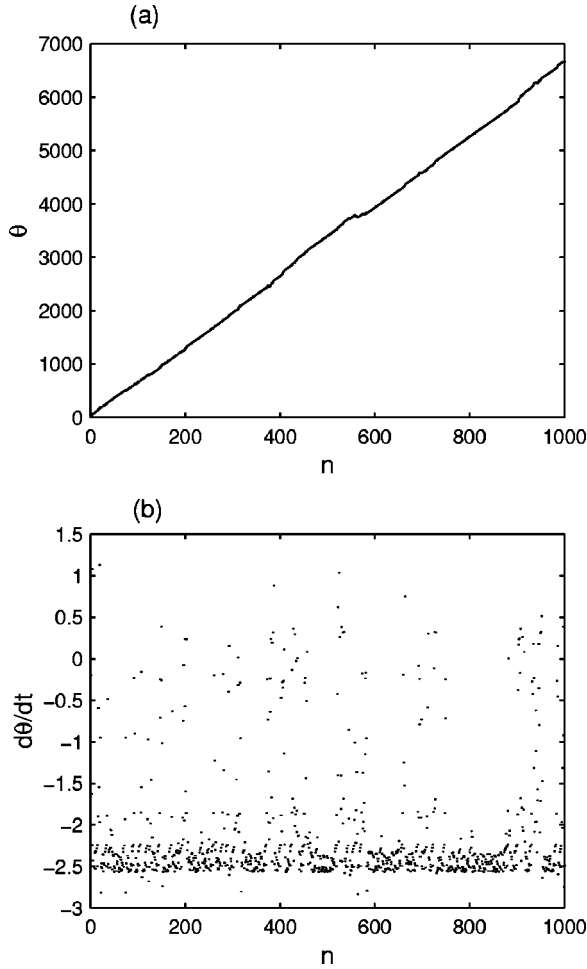


FIG. 13. Phase variables for the pendulum with bias  $p = 0.1188$ ,  $\omega = 0.4769$ ,  $f = 1.2$ , and  $\gamma = 0.2$ . (a) The motion is nearly linear. (b)  $\dot{\theta}$  showing a single intermittent region causing the nearly linear behavior in (a).

exhibits intermittency in the chaotic regions. In contrast to the intermittency shown earlier, for this case, there seems to be a single dominant intermittent region where the motion is nearly linear. The contribution to the motion during the

bursts is negligible as seen in Fig. 13. The effect of the bias on the intermittent region is shown in Fig. 14. At  $\omega = 0.47311$ ,  $\gamma = 0.2$ ,  $f = 1.2$ , and  $p = 0$ , there exist two intermittent regions as seen in Fig. 14(a). When a small bias  $p = 0.0005$  is added, one of the two intermittent regions is destroyed as seen in Fig. 14(b). Which of the two intermittent regions gets destroyed depends on the sign of the bias  $p$ . Since, there exists only one intermittent region the motion is nearly ballistic.

#### IV. SUMMARY AND CONCLUSION

The driven damped pendulum is a classic example of a nonlinear oscillator, whose behavior represents a large class of systems. We have studied diffusion process in this system and found both normal and anomalous diffusion. Divergence of the diffusion coefficient is found near certain bifurcation points of  $\omega$ . The diffusion coefficient near these points are shown to obey a power-law divergence with the exponent  $1/2$ . Near a crisis induced intermittency also power-law divergence of the diffusion coefficient is found. It has been shown that the large values of the diffusion coefficients near the bifurcation points is due to the existence of two intermittent regions. Further, the average lengths of these intermittent regions exhibit power-law divergence. It has been possible to show through random walk arguments that the divergence of the diffusion coefficient is similar to the divergence of the average laminar lengths. The effect of the intermittent regions in the case of the undamped pendulum is different. In this case, the contribution to the diffusion is due to the chaotic oscillations. The presence of the accelerator modes enhances the diffusion leading to the anomalous behavior. In the damped case, where two intermittent regions exist, however, the contribution due to the chaotic oscillations is small as compared to that by the intermittent regions leading to normal diffusion. In the case with bias near a periodic window, the periodicity is broken leading to a sequence of periodic and chaotic behavior as the bias is varied. In these cases, however, a single intermittent region exists leading to

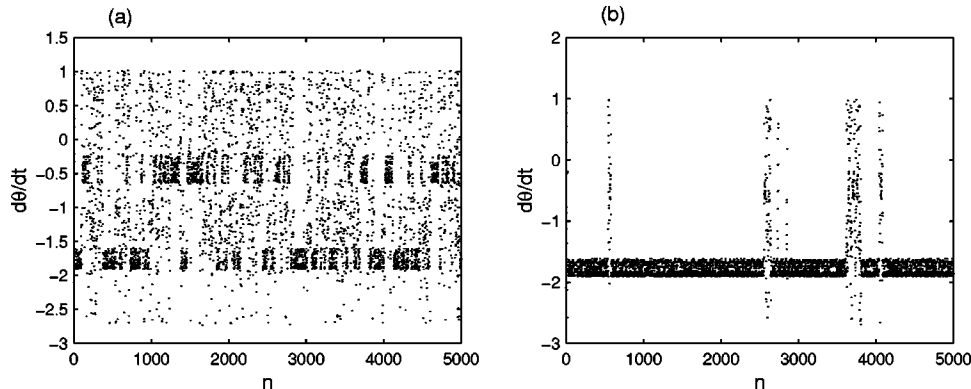


FIG. 14. Effect of bias on the intermittency at  $f = 1.2$ ,  $\omega = 0.47311$ , and  $\gamma = 0.2$ . The Poincaré plots are generated for a phase shift of  $\phi = 0.3\omega$  to accentuate the two intermittent regions. (a) For  $p = 0$ , the two intermittent regions exist similar to that shown in Fig. 6. (b) For  $p = 0.0005$ , one of the intermittent regions is destroyed. Which of the two intermittent regions gets destroyed depends on the sign of the bias. The consequent motion of the phase variable  $\theta$  is nearly linear and not diffusive.



nearly linear motion, which may be contrasted with the case without bias, where two possibly symmetric intermittent regions exist leading to the appearance of normal diffusion. The effect of bias seems to destroy one of the two intermittent regions producing nearly ballistic motion.

### ACKNOWLEDGMENT

The work of S.R. forms part of a research project sponsored by the Department of Science and Technology, Government of India.

- 
- [1] J. Haus and K.W. Kehr, Phys. Rep. **150**, 263 (1987).  
 [2] J.P. Bouchaud and A. Georges, Phys. Rep. **195**, 127 (1990).  
 [3] *Anomalous Diffusion From Basics to Applications*, edited by A. Pekalski and K. Sznajd-Weron, Lecture Notes in Physics Vol. 519 (Springer, New York, 1998).  
 [4] D.H. Zanette, e-print cond-mat/9905064.  
 [5] J.B. Weiss and E. Knobloch, Phys. Rev. A **40**, 2579 (1989).  
 [6] E. Weeks, J.S. Urbach, and H. Swinney, Physica D **97**, 291 (1996).  
 [7] D. del Castillo-Negrete, Phys. Fluids **10**, 576 (1998).  
 [8] R. Balescu, Phys. Rev. E **51**, 4807 (1995).  
 [9] G. Zimbardo and P. Veltri, Phys. Rev. E **51**, 1412 (1995).  
 [10] F.D. Angelo and R. Paccagnella, Phys. Plasmas **3**, 2353 (1996).  
 [11] P. Castiglione, A. Mazzino, and P. Muratore-Ginanneschi, Physica A **280**, 60 (2000).  
 [12] S. Rajasekar and V. Chinnathambi, Physica A **282**, 137 (2000).  
 [13] Hsen-Che Tseng, Peng-Ru Huang, Huang-Jung Chen, and Chin-Kun Hu, Physica A **281**, 323 (2000).  
 [14] M. Pettini, A. Vulpiani, J.H. Misguich, M. DeLeener, J. Orban, and R. Balescu, Phys. Rev. A **38**, 344 (1988).  
 [15] G.M. Zaslavsky, M. Edelman, and B.A. Niyazov, Chaos **7**, 159 (1997).  
 [16] A.A. Chernikov, B.A. Petrovichev, A.V. Rogalsky, R.N. Sagdeev, and G.M. Zaslavsky, Phys. Lett. A **144**, 127 (1990).  
 [17] D.K. Chaikovsky and G.M. Zaslavsky, Chaos **1**, 143 (1991).  
 [18] R. Ishizaki and H. Mori, Prog. Theor. Phys. **97**, 201 (1997).  
 [19] S. Benkadda, S. Kassibrakis, R.B. White, and G.M. Zaslavsky, Phys. Rev. E **55**, 4909 (1997).  
 [20] S.S. Abdullaev and K.H. Spatschek, Phys. Rev. E **60**, R6287 (1999).  
 [21] J.A. Blackburn and N. Gronbech-Jensen, Phys. Rev. E **53**, 3068 (1996).  
 [22] M.N. Popescu, Y. Braiman, F. Family, and H.G.E. Hentschel, Phys. Rev. E **58**, R4057 (1998).  
 [23] O. Yevtushenko, S. Flach, and K. Richter, Phys. Rev. E **61**, 7215 (2000).  
 [24] V. Latora, A. Rapisarda, and S. Ruffo, Phys. Rev. Lett. **83**, 2104 (1999).  
 [25] S. Flach, O. Yevtushenko, and Y. Zolotaryuk, Phys. Rev. Lett. **84**, 2358 (2000).  
 [26] The numerical scheme was also tested against the analytical solution wherever possible. For  $\omega=0$ ,  $\gamma=0$ , the absolute error was less than  $8.0E-6$  over 1000 drive cycles when a drive cycle was divided into 100 time steps. For  $\gamma=0$  and  $\omega=0.1$ , the absolute error was less than 0.013 for 5000 time steps per drive cycle and less than 0.15 for 100 time steps per drive cycle. The error is found to be maximum near the zeros of the solution and least near their extrema. In all cases, the numerically evaluated solution “shadows” the analytical solution.  
 [27] C. Grebogi, E. Ott, F. Romeiras, and J.A. Yorke, Phys. Rev. A **36**, 5365 (1987).  
 [28] The mean time between switching being quite large for the crisis induced intermittency, close to the bifurcation point longer orbit lengths are required to find normal diffusion. The small difference in the bifurcation point between what we have reported and that of Ref. [27] may be because of the same reason. This will result in a small change in the exponent.  
 [29] F. Reif, *Fundamentals of Statistical and Thermal Physics* (McGraw-Hill, New York, 1965).  
 [30] V. Mehra and R. Ramaswamy, Phys. Rev. E **53**, 3420 (1996).  
 [31] H.L.D. De, S. Cavalcante, and J.R. Rios Leite, Dyn. Stab. Syst. **15**, 35 (2000); Physica A **283**, 125 (2000).